JAN 3 9 1988

Multiple Collision Effects on the Antiproton

Production by High Energy Proton

(100 GeV - 1000 GeV)

BNL--40549

Hiroshi Takahashi

DE88 004873

James Powell

Brookhaven National Laboratory
Upton, New York 11973



Prepared for Rand Workshop, Oct. 6-9, 1987 on Antiproton Science and Technology.

DISTRIBUTION OF THIS DUCUMENT IS UNLIMITED

ABSTRACT

Antiproton production rates which take into account multiple collision are calculated using a simple model. Methods to reduce capture of the produced antiprotons by the target are discussed, including geometry of target and the use of a high intensity laser. Antiproton production increases substantially above 150 GeV proton incident energy. The yield increases almost linearly with incident energy, alleviating space charge problems in the high current accelerator that produces large amounts of antiprotons.

DISCLAIMER

This report was prepared as an account of work sponsored by an agency of the United States Government. Neither the United States Government nor any agency thereof, nor any of their employees, makes any warranty, express or implied, or assumes any legal liability or responsibility for the accuracy, completeness, or usefulness of any information, apparatus, product, or process disclosed, or represents that its use would not infringe privately owned rights. Reference herein to any specific commercial product, process, or service by trade name, trademark, manufacturer, or otherwise does not necessarily constitute or imply its endorsement, recommendation, or favoring by the United States Government or any agency thereof. The views and opinions of authors expressed herein do not necessarily state or reflect those of the United States Government or any agency thereof.

INTRODUCTION

The production of antiprotons which have been used for high energy physics and low energy antiproton annihilation studies has generally been carried out with a thin target of heavy metal. The thin target is used because it allows present collecting devices to capture only a small momentum bite of antiprotons, which are produced with wide momentum spread (1-6). In order to increase capture of antiprotons, lithium lens and horn type devices have been studied (1,2).

To produce and to collect the large amount of antiproton needed for performing antigravity experiments (7) or for spacecraft propulsion (8,9,10), several schemes for collecting antiprotons with large angular and momentum spread have been proposed. One such approach is a large solenoidal coil with high magnetic field (11). If antiprotons with large angular and momentum spread can be collected by these devices, then a thick target instead of a thin target can be used. In thick targets, secondary particles created by proton-nucleus collisions, such as pions or leading protons, can produce additional antiprotons in successive collisions.

In this paper, antiproton production due to multiple collisions is studied. The study indicates: (1) that above 150 GeV incident proton energy, substantial numbers of antiprotons are produced by successive collisions, and (2) antiproton yield increases almost linearly with incident proton energy. Cross Sections for antiproton, π^{\pm} meson and leading proton production.

In high energy P-P collisions, the sum of elastic and diffractive cross sections is about 20% of the total cross section. Protons which have been elastically or diffractively scattered have nearly as much energy as the incident proton. Such protons can produce antiprotons in successive collisions with the target. Protons produced as leading protons also have significant energy and can produce antiprotons in successive collisions.

The cross section of P(P,P)P is shown in Figure 1a as a function of $X = P_{\parallel}/P_{\parallel \max}$ (12). The longitudinal momentum spectrum for leading protons calculated from the cross section in the laboratory system is shown in Figure 2. As shown in the figure, the leading proton has a large longitudinal momentum.

The longitudinal momentum spectra of mesons produced from P-P collision (cross section of $P(P,\pi)X$) as a function of X is shown in Figure 1b and in the laboratory coordinate system in Figure 3. The mesons produced at X close to 1 are very small momentum. Antiproton production cross sections from the P-P and π^{\pm} -P collisions calculated from the Hojvat and Van-Ginnken's (1) empirical formula are shown in Figure 4. In the energy region less than 150 GeV incident particle energy, π^{\pm} mesons have larger antiproton production cross section than protons (see also ref. 13). This large antiproton production cross section of the pions contribute substantially to antiproton production. Roughly 1/3 of antiproton production is contributed each from proton, π^{+} and π^{-} particles.

Antiproton yield by multiple collisions.

Using these cross sections discussed in the previous section and assuming that no contribution from processes of $\pi^{\pm}(P,P)\pi^{\pm}$, and no capture of the produced antiproton in the collision with the nuclei, the yield of the antiproton from primarily, secondary, etc. collisions are calculated. Figure 5 shows the antiproton yield as function of incident proton energy.

The antiproton yield from multiple collisions becomes substantial above 150 GeV incident proton energy. At 200 GeV incident energy, antiproton yield due to secondary collisions is comparable to that from primary collisions. At 700 GeV incident energy, production from secondary collisions is about twice that from primary collisions.

For thin targets, where antiproton production is mostly due to primary collisions, antiproton yield above 150 GeV incident proton energy increases slowly. Yield is not proportional to incident energy and the most effective incident proton energy for antiproton production is a broad band around 200 GeV.

Total antiproton production due to multiple collisions is almost proportional to incident proton energy above 150 GeV. The energy cost for antiproton production does not change above this energy. Thus from the energy economy point of view, increasing incident proton energy does not benefit energy cost. However, when large amounts of antiproton are required, such as

for spacecraft propulsion, increasing incident proton energy reduces the beam current needed for a desired antiproton production rate. Reducing beam current alleviates problems associated with space charge in the high current accelerated beam.

Taking into account antiproton production from elastically and diffractively scattered protons and leading mesons in (π,P) collisions (which are neglected in this calculation), the yield of the antiproton becomes little higher than the value calculated here. However, the assumption that the produced antiprotons are not captured by target nuclei overestimates antiproton yield. The fraction of the produced antiprotons that are captured by target nuclei depends strongly on target geometry and incident beam profile. This issue is addressed in the section on targetry.

So far we have considered antiproton production in P-P collisions. It is expected that higher yields can be obtained from proton-high A nucleus collisions. The mechanism for antiproton production is taken as follows. When a quark in one nucleon collides with a quark in the other nucleon, a color string is stretched between these two quarks. Pions, baryons and antibaryons are then produced from the hadronization of the stretched string. The quark that collides with the other quark, which is called a wounded quark, does not collide with other quarks before leaving the nucleus. In the case of proton-proton collisions the usually only one quark-quark collision occurs and the probability of making second quark-quark collisions occur is very small. In the case of proton collisions with high A nuclei, the probability of second and third quark-quark collisions is high. Since the proton has two up quarks and one down quark, the number of stretched strings in a proton-high A nucleus collision is limited to 3.

In these calculations, pion and leading proton production in collision between a proton and a high A nucleus collision are calculated with the nucleus factor for antiproton production used by Hojvat and Van-Ginneken (1). Since the mechanism of leading proton production is different from antiproton production, this assumption overestimates antiproton yield in a multiple collision process. The calculated yield for a proton collision with a tungsten nucleus is shown in Figure 6. The antiproton yield for proton-tungsten

collisions is approximately a factor of three greater than for proton-proton collisions. The author was informed (2) that the empirical formula for antiproton production in proton-high A nuclei collisions overestimates the cross section at low $X = P_{\parallel}/P_{\parallel}$ max, compared to the experiment. As shown in the Figure 4, antiproton production for meson-proton collision is larger than for proton-proton collisions below 200 GeV. This is interpreted as follows. Pions are composed of a quark and antiquark. To produce antiprotons which are composed of two anti-up quarks and one anti-down quark, the quark of the pion is replaced by one antidiquark. In the proton-proton collision, however, three antiquarks must be created from the quark sea surrounding the colliding proton. Pion based production is thus energetically more favorable than the proton based production at low incident energies.

If pion could be accelerated in a short distance (because of its short rest frame lifetime of 2.6×10^{-8} sec) by laser acceleration, pions might be useful particles for producing antiprotons. In the multiple collision process, the favorable nature of pions for producing antiprotons is used effectively.

Targetry

We assumed in this calculation that the produced antiprotons are not captured by the target. The validity of this assumption depends on target geometry and beam profile. Evaluation of the absorption effect should be carried out using more detailed Monte Carlo calculations for various target geometries and beam profiles. One way to reduce absorption is to use a fine line solid target (i.e., small diameter) or a fine heavy metal jet target similar to that proposed for laser accelerators by Palmer (14,15). As shown in Figures 2,3, and 7 the longitudinal momentum of the produced antiproton is very small compared to the that of the leading proton and produced pions. The transverse momenta of these particles is on the order of 0.6 GeV/C. Produced antiprotons thus have more sideward emission than the leading proton and produced pions. Thus when high energy protons are injected into a slender long line target or liquid jet, the leading protons and the produced pions tend to stay inside the target and contribute to antiproton production by second and third multiple collisions. The produced antipions escape from the target and their capture by target nuclei is reduced.

By running a large electric current through a metallic target in the opposite sense to that of a lithium lens system (which focuses antiprotons), the produced antiprotons will be defocused and kicked away from the target (without much disturbance of the leading protons and pions), further reducing antiproton capture.

In addition, the proton distribution in the beam can be more intense in the periphery ("hollow beam"), allowing antiprotons produced near the target surface to easily escape. Another possibility for reducing antiproton capture, controlling, and slowing down antiprotons is a high intensity laser. Acceleration of charged particle using high intensity lasers has been proposed. Instead of using microwaves with a large cavity structure, laser irradiation of a suitably shaped micro structure can create strong electric fields which accelerate charged particles. Present technology can make micro structures of materials such as Si using lasers or electron beams, which would correspond to an electric field accelerating electrons on the order of 1 GV/m. To create an electric field of 1 GV/cm, a laser intensity of 2.7 x 10¹⁵ W/cm² is required. This is calculated from

$$I = \frac{C}{4\pi} \left(\frac{e}{2a_0^2} \right)^2 = 1.8 \times 10^{16} \text{ W/cm}^2$$
 (1)

where ao is the Bohr radius and the electric field of

$$E = (\frac{e}{2a^2}) = 2.57 \times 10^9 \text{ volt/cm}$$
 (2)

The laser intensity of 2.7 x 10^{15} W/cm² can be created using present technology.

For antiproton production, the high intensity laser would irradiate the micro structured surface of the target at the same time as the proton injection. The resultant antiprotons emitted transversely from the target surface would then be controlled by the electric field created by the laser irradiation. Surface structure design and laser intensity depend on the control

scheme for the antiprotons and the injected proton profile. It appears worthwhile to further pursue the concept of using a laser to control produced antiprotons and mesons.

The increased yield of antiprotons achievable with a multiple collision target greatly reduces cost of the product. Table 1 illustrates the cost potential using such targets for a range of power costs and accelerator/target costs.

. Table 1
Production Cost/Rate for Anti-Protons Using Multiple Collision Targets

Anti-proton Cost

Basis: lmA beam current (Avg) @ 1000 GeV (1000 MW)
50% efficient beam (electric to beam)
0.35 Tev beam energy per anti-proton produced
15% fixed changes per year
80% duty factor
100% collection of anti-protons

Accelerator/Target Capital Cost	(Million \$/mg) Power Cost	
	2¢/KWH	10¢/KWH
1 \$/watt	0.6	2.2
10 \$/watt	2.4	4.4
Production Rate = 700 mg/year (80% duty fac	etor)	

Anti-matter cost ranges from a low of 0.6 Million \$/milligram to a high of 4.4 M\$/mg, depending on input costs. Even the highest cost is probably acceptable.

Power costs range from 20/KWH to 100/KWH, depending on location (e.g., low cost hydro versus a fossil or nuclear plant). Previous cost estimates for the accelerator/target components of an accelerator-breeder system indicate approximately 1.5 \$/watt; the range of 1 to 10 \$/watt should cover the cost for an anti-proton system.

Most of the accelerator cost will be for rf power which can be estimated reasonably accurately. The actual target cost is more uncertain but it should be relatively low. The target probably will be a single fine jet of liquid lead. In practice, a number of separate targets will probably be required with beam splitting or switching to limit average current to the target. No single target would be able to handle 1000 megawatts of beam deposition.

The cost of the anti-proton collection and cooling system will probably decimate the target cost, and is difficult to estimate. However, the \$1 to \$10/watt range should provide sufficient margin for this component.

Total production rate from such a facility is 700 milligrams/year, which would provide for a large spacecraft propulsion effort. The facility power input requirement of 2000 megawatts is well within current U.S. capability.

CONCLUSION

This study shows that multiple collisions substantially increase antiproton production of 150 GeV and above incident proton energies. At 200 GeV, total production is approximately twice that of a single collision; above 200 GeV, yield increases almost linearly with incident proton energy. In order to make large amounts of antiproton, we can then increase incident proton energy instead of increasing beam current which creates a space charge problem in the beam. (This is not effective for thin targets, since yield is nonlinear with energy.) In the case of multiple collisions, capture of the produced antiprotons by the target is a potential problem. Capture of antiprotons can be avoided by using slender long targets or laser irradiation on a microstructured target surface. Evaluation of these approaches should be detailed Monte Carlo calculation, carried out by an investigation of how to collect antiprotons produced with large phase space.

In this paper, antiproton production from tungsten targets was calculated using a simple factor to describe the effect of target mass number on the antiproton production. This appears to overestimate both the leading proton production in the high energy range and antiproton production. This shortcoming should be corrected using models based on quark cascade theory.

In the case of a target with high A nuclei, many neutrons and antineutrons will be created along with the antiprotons. These are neglected in
this calculation. Antiproton production through high energy neutron and antineutron reactions should also be taken into account, along with antideuteron,
antitritium and strange particle production.

ACKNOWLEDGMENT

This research was carried out under the auspices of the U.S. Air Force Rocket Propulsion Laboratory. The authors would like to express their thanks to Profs. D. Cline and F. Mills for their valuable discussions.

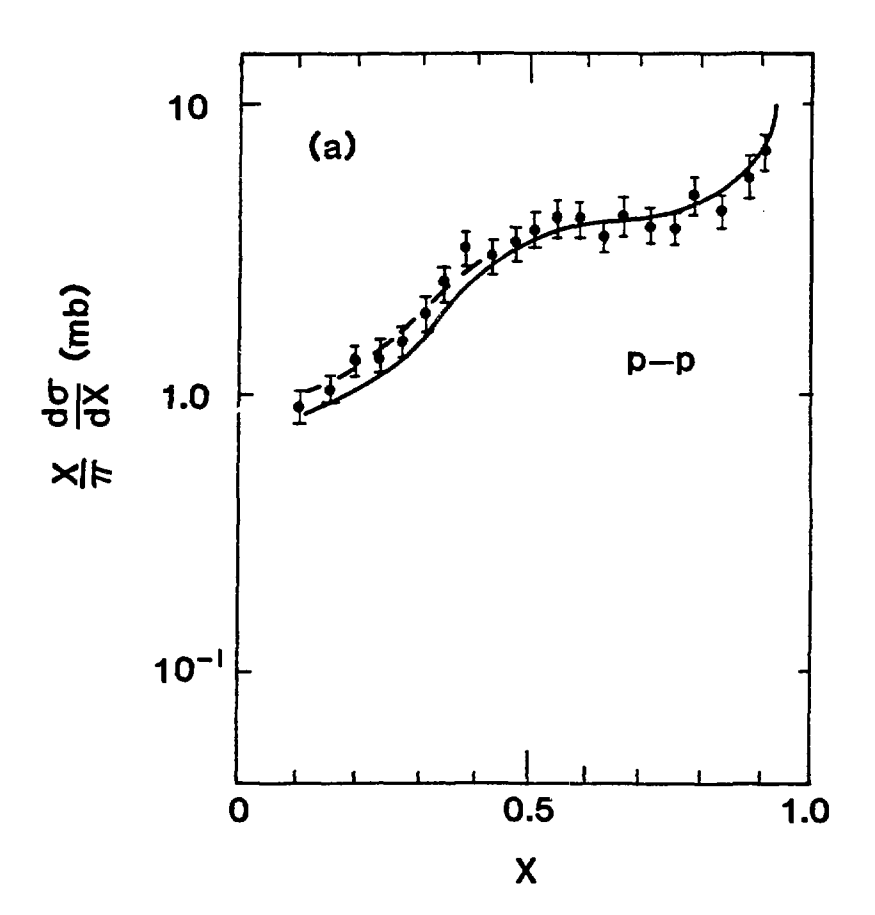
~ O -

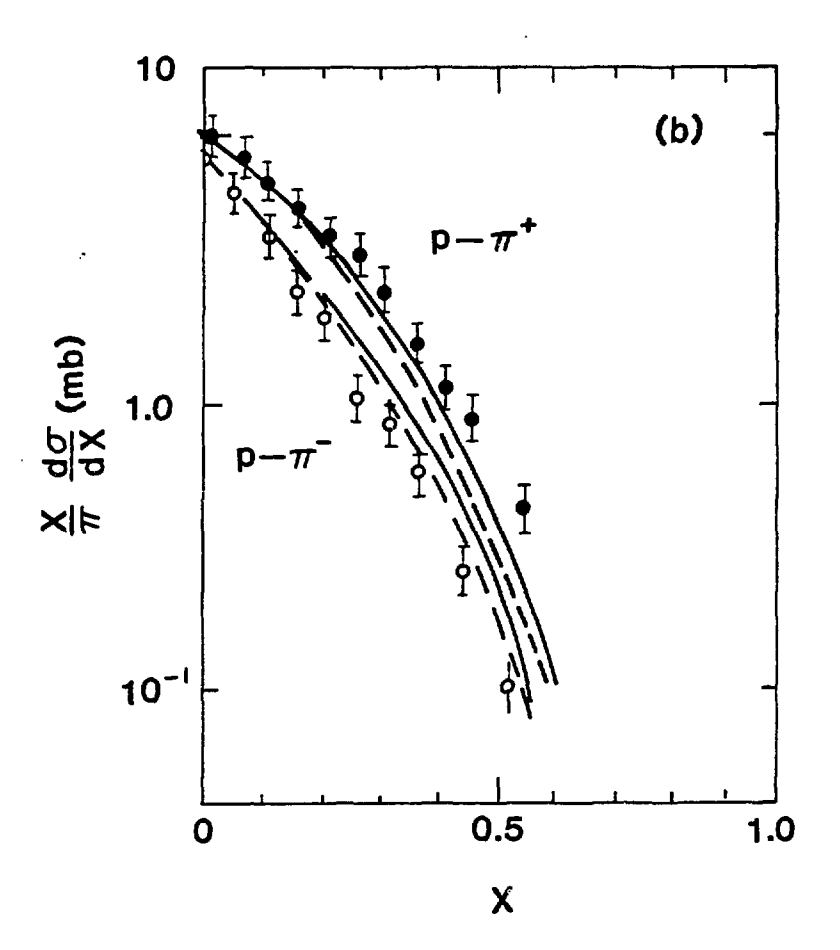
REFERENCES

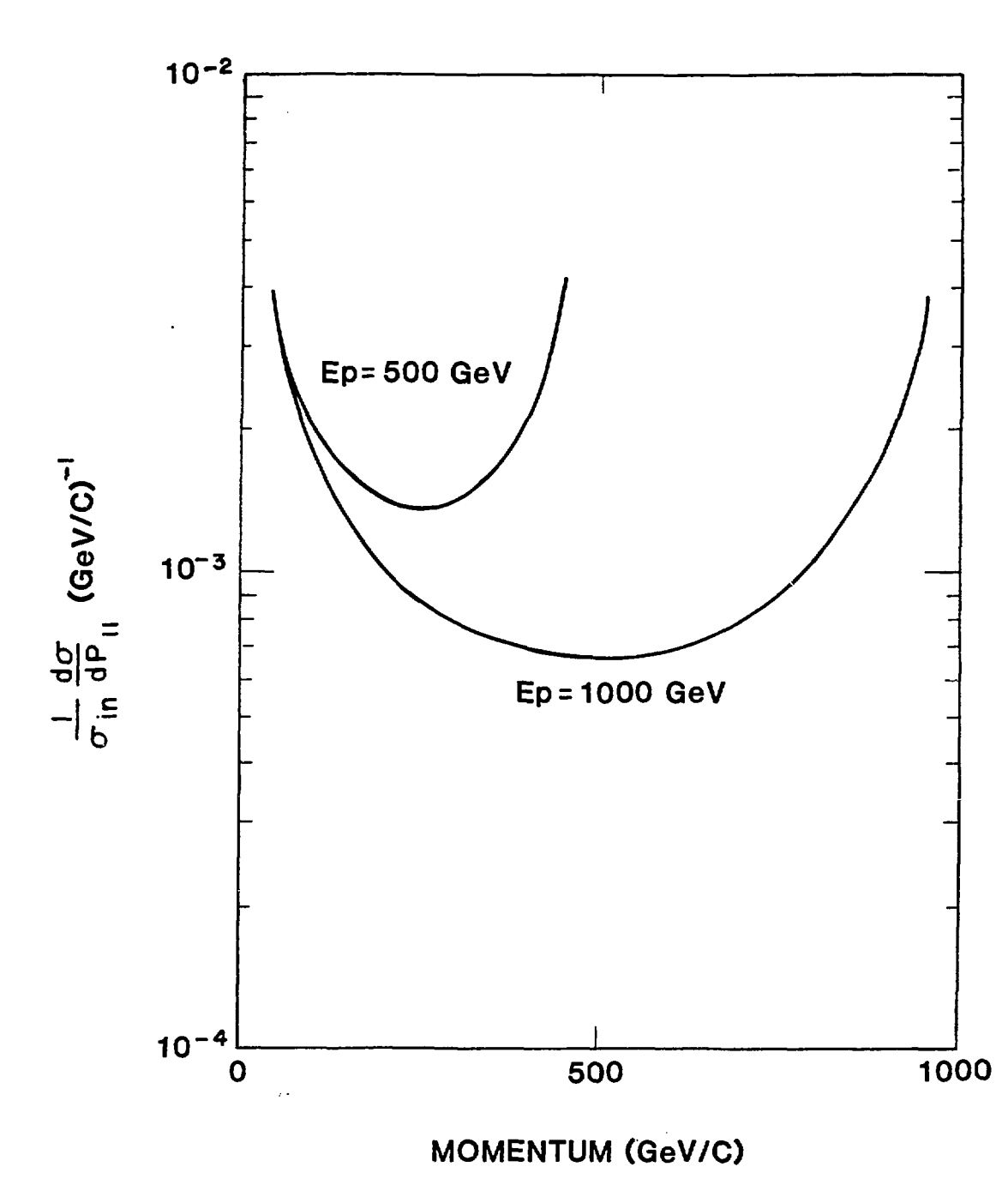
- C. Hojvat and A. VanGinneken, "Calculation of Antiproton Yields for the Fermi Antiproton Source," Nuclear Instrumentation and Methods, 206 (1983) 67-83.
- F.E. Mills, "Scaleup of Antiproton Production Facilities to 1 mg/yr,"
 Fermi National Accelerator Lab. Sept. 30 (1987).
- D. Cline, "The Development of Bright Antiproton Sources and High Energy Density Targetting," Proc. 11th Int. Conf. High Energy Accelerator, Geneva (1980).
- 4. T. Goldman, "Large Hadron Facility Adaptation," this proceeding.
- 5. D. Gill, "TRIUMF KAON Factory," this proceeding.
- 6. D. Lowenstein and Y. Lee, This proceeding
- 7. B.E. Bonner and M.M. Nieto, "Basic Physics Program for A. Low Energy Antiproton." This proceeding.
- 8. D.L. Morgar, "Concepts for the Design of an Antimatter Annihilation Rocket," Journal of the British Interplanetary Society, 35 (1982).
- 9. R.L. Forward, "Antiproton Annihilation Propulsion," AFRPL TR-85-034, Air Force Rocket Propulsion Laboratory. Edwards Air Force Base, CA, Sept. (1985).
- 10. B.W. Augenstein, "Concepts, Problems, and Opportunities for use in Annihilation Energy," An annotated Briefing on Near-Term RDT&E. To Assess Feasibility, RAND Note N-2302-AF/AC, Rand Corp., Santa Monica, CA 90406.
- 11. D. Cline, This proceeding
- 12. V.V. Anisovich, M.N. Kobrinsky, J. Nyiri, and Yu. M. Shabelski, "Quark Model and High Energy Collision," World Scientific, Singapore (1985).
- 13. B.N. Cassenti, "This Symposium".
- 14. R.B. Palmer, "A Laser-Driven Grating Linac," Particle Accelerators, 11 (1980), 81-90.
- 15. R.B. Palmer, N. Baggett, J. Claus, R. Fernow, et al., "Laser Plasma Linac," Proc. on Int. Conf. on Lasers 1984, San Francisco, CA. Nov. 26-30, 1984 (BNL-35737).

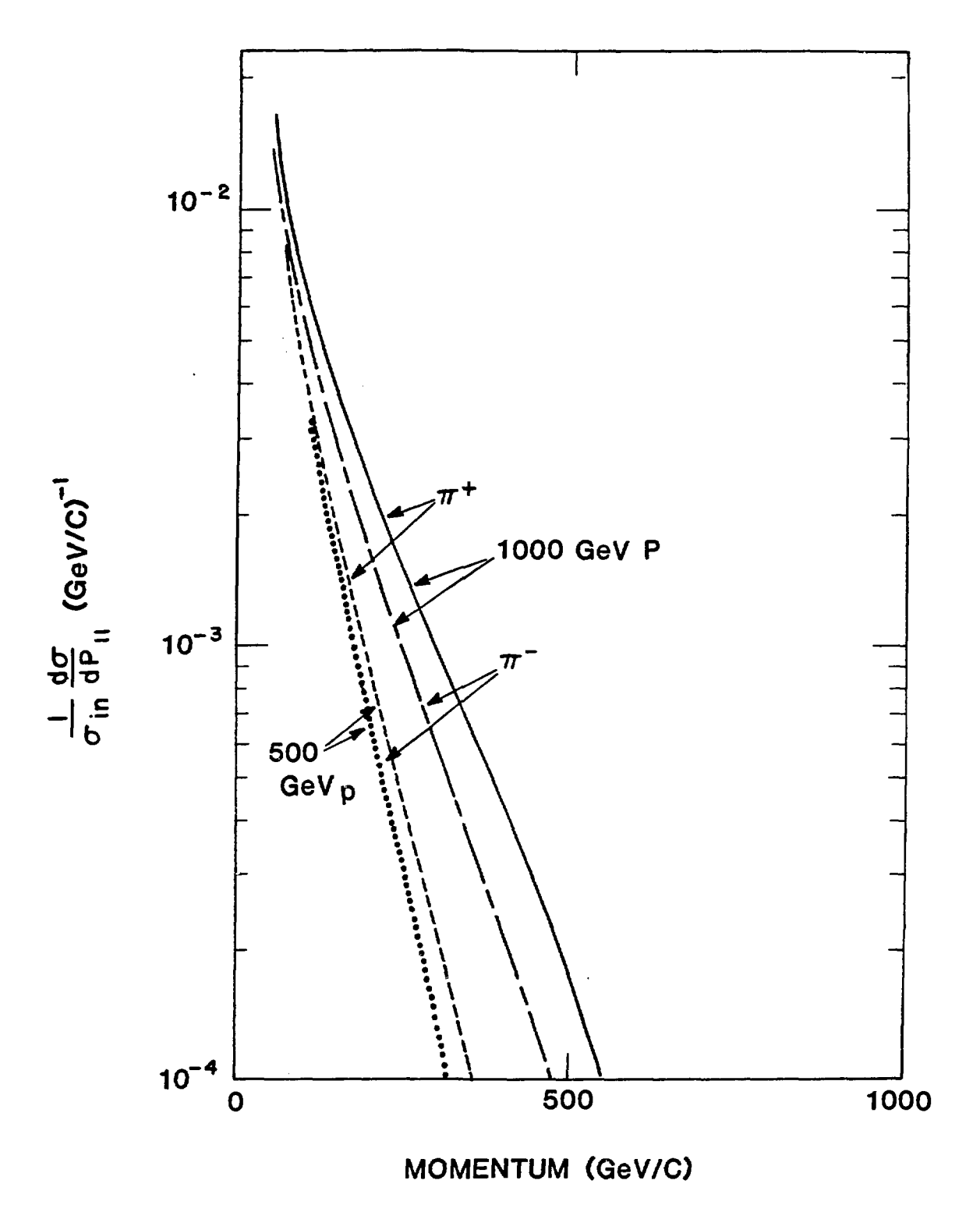
FIGURES

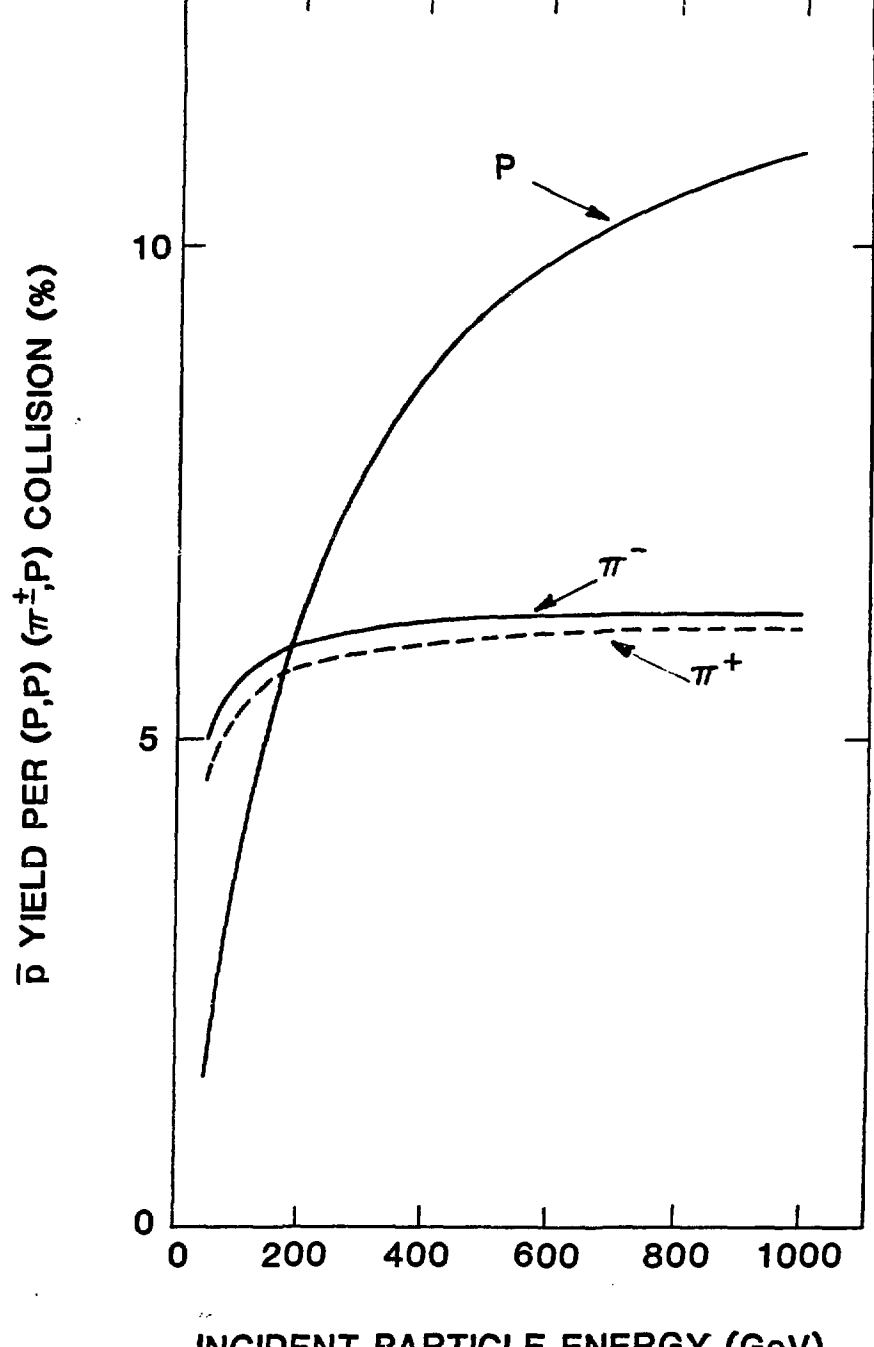
- la. The longitudinal center of mass momentum distribution of leading proton produced by the proton-proton collision, as function of Feyman $X = P_B/P_{Bmax}$.
- lb. The longitudinal center of mass momentum distribution of π^{\pm} meson produced by the proton-proton collision as function of Feyman X $P_{\parallel}/P_{\parallel max}$.
- 2. The longitudinal laboratory momentum spectra of leading proton produced by the proton-proton collision.
- 3. The longitudinal laboratory momentum spectra of the π^{\pm} mesons produced by the proton-proton collision.
- 4. The antiproton production rates in the proton-proton, and π^{\pm} mesons proton collision as functions of the incident proton and π^{\pm} meson energy.
- 5. The antiproton production rates in the multiple proton-proton collisions as the function of the proton energy initial incident.
- 6. The antiproton production rates in the multiple proton-tangsten collision as the function of the initial proton incident energy.
- 7. The laboratory system antiproton spectra produced by proton-proton and π^{\pm} meson proton collisions.











INCIDENT PARTICLE ENERGY (GeV)

